Hypersonic Leading Edge Problem: Wedges and Cones

MICHAEL L. SHORENSTEIN*
MIT, Cambridge, Mass.

An analysis is given for the viscous hypersonic flow past slender sharp wedges and unyawed cones. The leading edge or nose region treated encompasses the merged layer regime in which the shock thickness is not small in comparison with the viscous layer thickness but for which in the axisymmetric case the shock thickness is small in comparison with the radius of transverse shock curvature. A Navier-Stokes flow is assumed, and both the shock structure and viscous layer are taken to be locally-similar of boundary-layer type. The analysis follows that used by Shorenstein and Probstein for the corresponding flat plate problem. For axisymmetric cone flow, a modification of a transformation introduced by Probstein and Elliott is given to reduce the axisymmetric viscous layer equations including transverse curvature to "exactly" two-dimensional form. Results for the state conditions behind the shock, and the wall pressure and heat-transfer rate are found to be in good agreement with available experimental data.

Nomenclature

A = velocity ratio, u_s^*/U_∞
B = given by Eq. (15)
C = Chapman-Rubesin constant
C_1 = given by Eq. (17a)
C_2 = given by Eq. (17b)
c_p = specific heat at constant pressure
D = reduced density, ρ/ρ_∞
f = streamfunction given by Eq. (6)
$(f_\eta)_b$ = reduced slip velocity, u_{sl}^*/u_s^*
F = given by Eq. (35)
g = shear stress, $Nf_{\eta\eta}$
$g(0)$ = value of g at body surface
h = specific enthalpy, c_pT
H = total enthalpy
I = given by Eq. (11)
j = index taken to be zero for two-dimensional flow and unity for axisymmetric flow
L = arbitrary fixed reference length
M_∞ = freestream Mach number
n = normal coordinate for shock structure
N = given by Eq. (5)
p = static pressure
P = reduced pressure, $p/\rho_\infty U_\infty^2$
Pr = Prandtl number
$Q_1(j)$ = given by Eq. (22)
$Q_2(j)$ = given by Eq. (23)
$Q_3(j)$ = given by Eq. (34)
r = radius of transverse curvature, $r_b + y^* \cos\theta_b$
R = gas constant
$Re_{x^*,\infty}$ = local Reynolds number, $\rho_\infty U_\infty x^*/\mu_\infty$
St = Stanton number
T = static temperature
T_0 = freestream stagnation temperature
u, u^* = velocity component parallel to shock surface and to body surface, respectively (see Fig. 1)
U_∞ = freestream velocity
v, v^* = velocity component normal to shock surface and to body surface, respectively (see Fig. 1)
$\bar{v}$ = transformed normal velocity given by Eq. (2a)
V = reduced velocity, v/U_∞
W = reduced velocity, u/U_∞
x^*, y^* = coordinate along body surface and normal to body surface, respectively (see Fig. 1)
$\bar{x}, \bar{y}$ = transformed coordinates given by Eq. (2a)
α = inverse Reynolds number $(\rho_\infty U_\infty r_b/\mu_\infty)^{-1}$
γ = specific heat ratio
Δ_s = shock thickness
ζ = stretched normal coordinate for shock structure, Eq. (18)
η = stretched normal coordinate for viscous layer, Eq. (6)
η_b = transformed location of the body surface for the case of slip
η_s = location of the shock surface
θ_b = body surface inclination angle with respect to the freestream
θ_s = shock surface inclination angle with respect to the body surface
Θ = reduced enthalpy given by Eq. (6)
μ = viscosity
$\bar{\mu}$ = given by transformation Eq. (2b)
ξ = transformed coordinate along body surface given by Eq. (6)
ρ = density
$\sigma(j)$ = cross section of streamtube incident to viscous layer
Φ = reduced enthalpy given by Eq. (18)
$\bar{\chi}_\infty$ = interaction parameter, $M_\infty^3(C/Re_{x^*,\infty})^{1/2}$

Subscripts
b = condition at the body surface
nsl = quantity obtained from no-slip solution
s = condition at the shock surface
sl = quantity obtained from slip solution
η = derivative with respect to η
∞ = condition at the freestream

Received April 28, 1971; revision received February 17, 1972. The author wishes to thank sincerely R. F. Probstein of MIT for his support during the course of this investigation and for his valuable suggestions and criticisms. This research was supported by the Advanced Research Projects Agency and was technically administered by the Office of Naval Research under Contract N00014-0204-0040, ARPA Order 322.

* Research Assistant.

I. Introduction

SEVERAL classes of continuum flow models have been investigated recently for treating the hypersonic flow past sharp bodies upstream of the strong interaction regime in the merged layer where the shock thickness must be considered finite in comparison with the viscous layer thickness. One class[1-3] applies the full Navier-Stokes equations in finite-difference form in order to determine to what extent a continuum may meaningfully describe the flowfield in the merged layer. This complex scheme requires rather large computer storage space.

Another class of merged layer models[4-6] uses the Navier-Stokes equations but assumes "local similarity" to apply in both the viscous layer and shock wave, that is, streamwise variations of all properties are taken to be sufficiently small, so that the Navier-Stokes equations, when applied locally, can be approximated by ordinary differential equations. This description of the merged viscous shock layer is obtained from locally-similar solutions "patched" at the interface between the outer shock structure portion and the inner viscous layer portion in which the equations are taken to be of boundary-layer type with normal pressure gradient effects neglected. Results in Ref. 6 from such a merged layer model for a flat plate have compared well with experimental data.[7-9] The theoretical calculations have shown the relative importance of several rarefaction effects over a cold sharp flat plate aligned parallel to the hypersonic freestream. Dominant among these

effects was shown to be the finite shear at the interface between the back of the shock and the outer edge of the viscous layer. The effect of including velocity slip and temperature jump at the body surface was shown to be smaller but non-negligible, while the effect of including longitudinal shock curvature was found in comparison to be negligible.

The present analysis extends this flat plate continuum merged layer model of Ref. 6 to wedge and axisymmetric conical flows by investigating the additional effects of body slope and, for conical flow, the effects of axial symmetry and transverse curvature effects. Longitudinal shock curvature effects are neglected as small based on the results of Ref. 6. Body slope effects are characterized by the parameter θ_b, where θ_b is the half angle of the wedge or unyawed cone. The analysis is extended only to slender bodies with $\theta_b \ll 1$ for which the normal component of the viscous layer velocity can be neglected compared to the tangential component. This restriction is introduced in order to solve the viscous layer problem by the method of Ref. 6.

In the axial symmetric case, a modification of a Mangler type transformation given by Probstein and Elliott[10] is introduced to reduce the axisymmetric viscous layer equations to an "exactly" two-dimensional form. The modification involves a transformation applied to the viscosity coefficient, and this transformation is shown to include the effects of transverse curvature characterized by the parameter $M_\infty\alpha$. Here α is an inverse Reynolds number based on the body radius r_b of transverse curvature, and M_∞ is the freestream Mach number. A new term proportional to $M_\infty\alpha$ is found to modify the reduced viscous layer momentum equation of Ref. 6 and is shown to account for transverse curvature effects.

For the present investigation, two regimes of $M_\infty\alpha$ are distinguished: I, a regime immediately adjacent to the sharp nose where $M_\infty\alpha \gtrsim 1$ and II, a regime downstream of the sharp nose where $M_\infty\alpha \ll 1$. Only the second regime is treated here. This restriction is introduced to obtain a simple closed form shock structure solution by a method analogous to Ref. 6. In the conical shock structure equations, transverse shock curvature terms are of order Δ_s/r_s where Δ_s is the shock thickness and r_s is the radius of transverse shock curvature. It is found that if $M_\infty\alpha \ll 1$, then terms of order Δ_s/r_s are negligible compared to the other terms in the shock structure equations. These equations can then be reduced to the form of the "zero-order" shock equations solved in Ref. 6.

II. Viscous Layer

As in Ref. 6, the merged shock layer is described by a viscous layer of boundary layer type patched at an outer interface (the "shock surface") to a thick shock structure. The velocity and state variables from the solution of the viscous layer equations are matched locally at the shock surface to the corresponding quantities from the solution of the shock structure equations.

The governing equations for the viscous layer written in the local body-centered coordinate frame (x^*, y^*) depicted in Fig. 1 are

$$\frac{\partial}{\partial x^*}(r^j\rho u^*) + \frac{\partial}{\partial y^*}(r^j\rho v^*) = 0 \tag{1a}$$

$$\rho\left(u^*\frac{\partial u^*}{\partial x^*} + v^*\frac{\partial u^*}{\partial y^*}\right) = -\frac{dp}{dx^*} + \frac{\partial}{\partial y^*}\left(\mu\frac{\partial u^*}{\partial y^*}\right) + j\frac{\mu}{r}\frac{\partial r}{\partial y^*}\frac{\partial u^*}{\partial y^*} \tag{1b}$$

$$\rho\left(u^*\frac{\partial h}{\partial x^*} + v^*\frac{\partial h}{\partial y^*}\right) = u^*\frac{dp}{dx^*} + \frac{1}{Pr}\left[\frac{\partial}{\partial y^*}\left(\mu\frac{\partial h}{\partial y^*}\right) + j\frac{\mu}{r}\frac{\partial r}{\partial y^*}\frac{\partial h}{\partial y^*}\right] + \mu\left(\frac{\partial u^*}{\partial y^*}\right)^2 \tag{1c}$$

where $j = 0$ for two-dimensional flow and $j = 1$ for axisymmetric flow, with $r(x^*, y^*) = r_b(x^*) + y^*\cos\theta_b$ the local radius of transverse curvature for the case of axisymmetric flow with θ_b the body slope relative to the freestream direction. The tangential and normal components of velocity are u^* and v^*, respectively (see

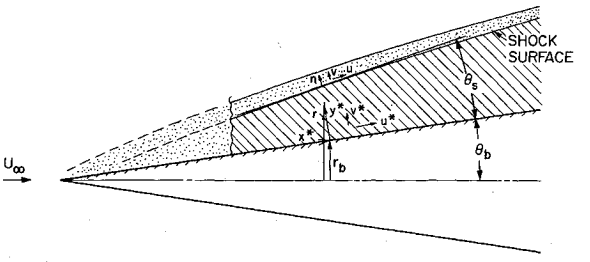

Fig. 1 Merged layer detail.

Fig. 1), h is the specific enthalpy, p is the pressure, μ is the viscosity, and Pr is the Prandtl number taken to be a constant.

Probstein and Elliott[10] introduced a generalized Mangler transformation which reduced Eqs. (1) to an almost two-dimensional form by applying the transformations

$$\begin{aligned} &d\bar{x} = (r_b/L)^{2j}\,dx^*, \quad \partial/\partial x^* = (r_b/L)^{2j}\,\partial/\partial\bar{x} + j(\partial\bar{y}/\partial x^*)\,\partial/\partial\bar{y} \\ &d\bar{y} = (r/L)^j\,dy^*, \quad \partial/\partial y^* = (r/L)^j\,\partial/\partial\bar{y} \\ &\bar{v} = (rL/r_b^2)^j\,v^* + j[(L/r_b)^2\,\partial\bar{y}/\partial x^*]u^* \end{aligned} \tag{2a}$$

where L is an arbitrary fixed reference length. By also introducing the transformation

$$\bar{\mu} = (1 + 2jL\,\bar{y}\cos\theta_b/r_b^2)\mu \tag{2b}$$

Eq. (1) can be reduced "exactly" to two-dimensional form. This follows from the fact that θ_b and r_b are functions of $\bar{x}$ only, so that Eq. (1) when transformed by means of Eqs. (2) give the homogeneous system

$$\partial(\rho u^*)/\partial\bar{x} + \partial(\rho\bar{v})/\partial\bar{y} = 0 \tag{3a}$$

$$\rho(u^*\,\partial u^*/\partial\bar{x} + \bar{v}\,\partial u^*/\partial\bar{y}) - \partial(\bar{\mu}\,\partial u^*/\partial\bar{y})/\partial\bar{y} + dp/d\bar{x} = 0 \tag{3b}$$

$$\rho(u^*\,\partial h/\partial\bar{x} + \bar{v}\,\partial h/\partial\bar{y}) - (1/Pr)\,\partial(\bar{\mu}\,\partial h/\partial\bar{y})/\partial\bar{y} - \bar{\mu}(\partial u^*/\partial\bar{y})^2 - u^*\,dp/d\bar{x} = 0 \tag{3c}$$

which are "two-dimensional" in form. It must be pointed out, however, that the parameter $\bar{\mu}$, although having the dimensions of a viscosity, is not a true state variable since it depends not only upon temperature but also on the geometry of the system. Still, Eqs. (3) can be interpreted as *mathematically* analogous to the equations of two-dimensional flow. Furthermore, Eqs. (3) can be solved by the method used in the viscous layer problem of Ref. 6 if $\bar{v}$ can be taken as small compared to u^*. The present work therefore extends the merged layer model of Ref. 6 only to slender bodies ($\theta_b \ll 1$) for which the viscous layer streamline curvature $\partial y^*/\partial x^*$ can be ignored and for which v^* is negligibly small compared to u^*. For such bodies, by Eq. (2a), $\bar{v} \ll u^*$.

With the governing equations in two-dimensional form and with $\bar{v} \ll u^*$, the analysis can more directly parallel that of Ref. 6. Following this reference, the viscous layer adjacent to the body is assumed locally similar, and for a calorically perfect gas with a Prandtl number of unity, Eqs. (3b) and (3c) then reduce to

$$(Nf_{\eta\eta})_\eta + ff_{\eta\eta} = 0 \tag{4a}$$

$$(N\Theta)_\eta + f\Theta_\eta = 0 \tag{4b}$$

where

$$N = \rho\bar{\mu}/\rho_b\bar{\mu}_b \tag{5}$$

and where the dimensionless independent and dependent variables are

$$\eta = \frac{u_s^*}{(2\xi)^{1/2}}\int_0\rho\,d\bar{y}; \qquad \xi(\bar{x}) = \int_0\rho_b\bar{\mu}_b u_s^*\,d\bar{x}$$

$$f(\eta) = \int_0\frac{u^*}{u_s^*}\,d\eta; \qquad \Theta(\eta) = \frac{\bar{H} - \bar{H}_b}{\bar{H}_s - \bar{H}_b} \tag{6}$$

Here $\bar{H}$ is the total enthalpy in the barred system (with $\bar{v} \ll u^*$) and the subscripts "s" and "b" denote quantities at the shock surface and body surface, respectively.

Following Ref. 6, we first consider the problem neglecting velocity slip and temperature jump at the body surface. With the body temperature T_b constant, the boundary conditions are then

$$f = f_\eta = 0, \quad \Theta = 0 \quad \text{at} \quad \eta = 0$$
$$f_\eta = 1, \quad \Theta = 1 \quad \text{at} \quad \eta = \eta_s \tag{7}$$

Consider now the energy equation (4b) which is satisfied by the Crocco integral $\Theta = f_\eta$. From the definition of total enthalpy (with $\bar{v} \ll u^*$)

$$T/T_b = (1 - f_\eta)[1 + A^2(T_0/T_b)f_\eta] \tag{8}$$

where

$$A(\bar{x}) = u_s^*/U_\infty \tag{9}$$

with U_∞ the freestream velocity. For the hypersonic conditions considered, the freestream stagnation temperature T_0 is given by $T_0 = U_\infty^2/2c_p$.

Consider next the viscous layer momentum Eq. (4a). An expression for N is sought so that Eq. (4a) can be expressed in terms of the streamfunction $f(\eta)$ and its derivatives and in terms of the local boundary conditions at the shock surface and the body. As shown in Pan and Probstein,[4] the normal pressure gradient across the viscous layer is negligible when viscous layer streamline curvature is negligible. Thus, by $p = \rho RT$, $\rho_b/\rho = T/T_b$ so that from the definition of η[Eq. (6)] it follows from Eq. (8) that at any given $\bar{x}$

$$\bar{y} = [(2\xi)^{1/2}/\rho_b u_s^*]\, I(\eta) \tag{10}$$

where

$$I(\eta) = \int_0^\eta (1 - f_\eta)[1 + A^2(T_0/T_b)f_\eta]\, d\eta \tag{11}$$

Hence, from Eq. (10) and from the definition of $\bar{\mu}$ [Eq. (2)]

$$\bar{\mu}/\mu = 1 + BI(\eta) \tag{12}$$

where B is a function of the boundary conditions at $\eta = 0$ and $\eta = \eta_s$. Since $N = (\rho/\rho_b)(\bar{\mu}/\bar{\mu}_b) = (T_b/T)(\bar{\mu}/\mu_b) = (T_b/T)(\mu/\mu_b)(\bar{\mu}/\mu)$ and if a viscosity-temperature relation of the form $\mu \sim T^{1/2}$ is assumed, then by Eq. (12)

$$N = (T_b/T)^{1/2}\,[1 + BI(\eta)] \tag{13}$$

To complete this expression for N, we now obtain B in terms of the local boundary conditions at the shock surface and the body. This is done by first applying local conservation of mass flux across the shock and into the viscous layer by use of

$$\rho_\infty U_\infty \sigma(j) = (2\pi L)^j \int_0^{\bar{y}_s} \rho u_s^*\, d\bar{y} = (2\pi L)^j (2\xi)^{1/2} f(\eta_s) \tag{14a}$$

where $\sigma(j)$ is the cross section of the incident streamtube given by

$$\sigma(0) = [1 + \tfrac{1}{2}(\cot\theta_s - \tan\theta_b)\sin 2\theta_b]\, y_s^*/\cos\theta_b \tag{14b}$$
$$\sigma(1) = \pi r_s^2 \tag{14c}$$

Then, setting $y_s^* = x^* \tan\theta_s$ and from the definitions of $\bar{x}$ [Eq. (2)] of $\xi(\bar{x})$ [Eq. (6)], and of $\bar{\mu}$ [Eq. (2b)], it can be shown that

$$B = \{8j\mu_b/3\mu_\infty \tan\theta_b[1 + (\tan\theta_s/\tan\theta_b)]^2\}\, f(\eta_s)\alpha \tag{15}$$

Here α is the inverse Reynolds number $(\rho_\infty U_\infty r_b/\mu_\infty)^{-1}$ based on freestream conditions and the local radius $r_b(x^*)$ of transverse body curvature. From Eq. (15), B vanishes for two-dimensional flow ($j = 0$).

From the energy equation in the form of Eq. (8), from $\mu \sim T^{1/2}$, and from Eqs. (13) and (15) which together relate the parameter N to the streamfunction $f(\eta)$, to its derivatives, and to the local boundary conditions on the viscous layer, the viscous layer momentum Eq. (4a) now reduces to

$$\left[\frac{\{1 + C_2 I(\eta)\}f_{\eta\eta}}{\{(1 - f_\eta)[1 + C_1 f_\eta]\}^{1/2}}\right]_\eta + ff_{\eta\eta} = 0 \tag{16}$$

where

$$C_1 = A^2(T_0/T_b) \tag{17a}$$

$$C_2 = \left\{8j\left(\frac{\gamma - 1}{2}\frac{T_b}{T_0}\right)^{1/2} f(\eta_s)/3\tan\theta_b[1 + (\tan\theta_s/\tan\theta_b]^2\right\} M_\infty\alpha \tag{17b}$$

Equation (16) differs from the reduced viscous layer momentum equation of Ref. 6 only by the appearance of the new term $C_2 I(\eta)$. This term introduces the effects of transverse curvature characterized by the parameter $M_\infty\alpha$, and it vanishes for the case of two-dimensional flow. For the case of axial symmetric flow, only the regime $M_\infty\alpha \ll 1$ is treated in this work. The reason for this will be discussed in conjunction with the shock structure analysis.

Now, if C_1 and C_2 were to be treated as parameters, then for each value of $(f_{\eta\eta})_b$ greater than the value which gives the boundary-layer solution ($\eta_s \to \infty$), a viscous layer solution would be obtained with finite shear (proportional to $Nf_{\eta\eta}$) at the shock surface $\eta = \eta_s$ where $f_\eta = u^*/u_s^* = 1$. The shock surface coordinates x^*, y_s^* corresponding to η_s are determined by 1) employing Eq. (14a) which states that mass flux into the viscous layer between the body and shock surface is conserved and 2) by matching the velocity u^* and its gradient $\partial u^*/\partial y^*$ obtained with finite shear at the outer edge of the viscous layer to the respective quantities obtained at the inner edge of the shock from the shock structure solution.

III. Shock Structure

To solve the shock structure equations, the following reduced dimensionless variables are introduced:

$$\zeta = \int_0^\infty \frac{\rho_\infty U_\infty}{\mu}\left(\frac{r_s}{r}\right)^j dn, \quad W = \frac{u}{U_\infty}, \quad V = \frac{v}{U_\infty}$$
$$P = p/\rho_\infty U_\infty^2, \quad D = \rho/\rho_\infty, \quad \Phi = (h + \tfrac{1}{2}v^2)/U_\infty^2 \tag{18}$$

The dimensionless forms of the continuity and tangential momentum equations can then be written

$$D_s V_s = [1 + j(\Delta_s/r_s)]\, D_\infty V_\infty \tag{19a}$$
$$\partial^2 W/\partial\zeta^2 - D_s V_s(\partial W/\partial\zeta) = 0 \tag{19b}$$

where $\Delta_s \equiv (r_\infty - r_s)$ denotes shock thickness. Equations (19) differ from the "zero-order" shock transition equations of Ref. 6 only by the appearance of the transverse shock curvature parameter Δ_s/r_s. If however $M_\infty\alpha \ll 1$, then $\Delta_s/r_s \ll 1$ and a simple closed form solution to Eqs. (19) can be readily obtained analogous to the "zero-order" shock solution in Ref. 6. In the present model, $M_\infty\alpha \ll 1$ is satisfied and transverse shock curvature terms are neglected as small in the shock structure equations. Equations (19) then become

$$D_s V_s = D_\infty V_\infty \tag{20a}$$
$$\partial^2 W/\partial\zeta^2 - D_s V_s(\partial W/\partial\zeta) = 0 \tag{20b}$$

and in similar manner the normal momentum equation and the energy equation for the shock structure become

$$D_s V_s(\partial V/\partial\zeta) + \partial P/\partial\zeta - \tfrac{4}{3}(\partial^2 V/\partial\zeta^2) = 0 \tag{20c}$$
$$D_s V_s\frac{\partial\Phi}{\partial\zeta} - \tfrac{4}{3}\frac{\partial^2\Phi}{\partial\zeta^2} + D_s V_s W\frac{\partial W}{\partial\zeta} - \frac{\partial W}{\partial\zeta}\left(W\frac{\partial W}{\partial\zeta}\right) = 0 \tag{20d}$$

The shock structure is taken to extend from the outer edge of the viscous layer $\zeta = 0$ to the freestream $\zeta \to \infty$. At the shock surface, the shock structure flow variables and their normal gradients are required to match the corresponding viscous layer values at $\eta = \eta_s$ as given by the solution to Eq. (16).

Following Ref. 6, we now illustrate this matching procedure at the shock surface for the case of the finite tangential shear stress $\mu_s(\partial u^*/\partial y^*)_s$. In terms of viscous layer variables, this stress may be written

$$[\mu(\partial u^*/\partial y^*)]_s = Q_1(j)\, Q_2(j)\, \rho_\infty U_\infty^2 A(Nf_{\eta\eta}/2f)_s \tag{21}$$

where

$$Q_1(j) = \begin{cases} [1 + \tfrac{1}{2}(\cot\theta_s - \tan\theta_b)\sin 2\theta_b]\,(\tan\theta_s/\cos\theta_b) & \text{for } j = 0 \\ [1 + (\tan\theta_s/\tan\theta_b)]^2\,(3L/2x^*) & \text{for } j = 1 \end{cases} \tag{22}$$

$$Q_2(j) = \left\{ \frac{\sin\theta_b(1 + \tan\theta_s/\tan\theta_b)(x^*/L)}{1 + 2(\tan\theta_s/\tan\theta_b)[1 + (\tan\theta_s/2\tan\theta_b)]} \right\}^j \quad (23)$$

On the other hand, at the inner edge of the shock, the shear is

$$\left(\mu\frac{\partial u^*}{\partial y^*}\right) = \rho_\infty U_\infty^2 \left(\frac{\partial W}{\partial \zeta}\right)_s \left(\frac{\partial n}{\partial y^*}\right)_s \left(\frac{\partial u^*}{\partial u}\right)_s = \rho_\infty U_\infty^2 \left(\frac{\partial W}{\partial \zeta}\right)_s \quad (24)$$

with the subscript "s" here denoting conditions at $\zeta = 0$. Equating Eq. (21) to Eq. (24)

$$(\partial W/\partial\zeta)_s = Q_1(j)\,Q_2(j)\,A(Nf_{\eta\eta}/2f)_s \quad (25)$$

This matching of viscous layer solution to shock structure solution at the shock surface is shown next for the case of the shock surface velocity u_s^*. First, recognizing from Fig. 1 that at the freestream $W_\infty = \cos(\theta_s + \theta_b)$ and $V_\infty = -\sin(\theta_s + \theta_b)$, *and* and at the shock surface $W_s = (u_s^*/U_\infty)(u_s/u_s^*) = A\cos\theta_s$, the tangential momentum Eq. (20b) is integrated once with the result

$$(\partial W/\partial\zeta)_s = [\cos(\theta_s + \theta_b) - A\cos\theta_s]\sin(\theta_s + \theta_b) \quad (26)$$

Substituting Eq. (26) into Eq. (25) and solving for the reduced velocity A at the shock surface

$$A = \frac{u_s^*}{U_\infty} = \left\{ \frac{\cos\theta_s}{\cos(\theta_s + \theta_b)} + \frac{2Q_1(j)Q_2(j)}{\sin[2(\theta_s + \theta_b)]}\left(\frac{Nf_{\eta\eta}}{2f}\right)_s \right\}^{-1} \quad (27)$$

For the case of flat plate flow $j = 0$ and $\theta_b = 0$, Eq. (27) reduces to the result of Ref. 6.

The shock angle in terms of the density and pressure behind the shock is obtained next by integrating the normal momentum Eq. (20c) once and applying freestream boundary conditions, neglecting the gradient term $(\partial V/\partial\zeta)_s$ as small compared to V_s (see Ref. 5) and eliminating V_s by means of Eq. (20a). The result is

$$\sin^2(\theta_s + \theta_b) = D_s(P_s - 1/\gamma M_\infty^2)/(D_s - 1) \quad (28)$$

In order to obtain the density ratio across the shock, another expression for $\sin^2(\theta_s + \theta_b)$ is found. Integrating the tangential momentum equation (20b) twice to obtain the velocity profile $W(\zeta)$, substituting this profile into the energy Eq. (20d) and integrating twice, the reduced enthalpy Φ_s is obtained. Finally, substituting V_s from Eq. (20a) and Φ_s into the reduced equation of state

$$P_s = [(\gamma - 1)/2\gamma]\,D_s(2\Phi_s - V_s^2) \quad (29)$$

and equating the resulting expression for $\sin^2(\theta_s + \theta_b)$ to Eq. (28), the density ratio is

$$D_s = \frac{\rho_s}{\rho_\infty} = \frac{[(\gamma + 1)/(\gamma - 1)]\,P_s + 1/\gamma M_\infty^2}{P_s + [1 - A\cos\theta_s/\cos(\theta_s + \theta_b)]^2 + (1/\gamma M_\infty^2)(\gamma + 1)/(\gamma - 1)} \quad (30)$$

The reduced pressure $P_s[\eta_s(\bar{x})]$ at the shock surface has, as stated before in conjunction with Eq. (10), been assumed equal to the reduced pressure $P_b(\bar{x})$ on the body at the same value of $\bar{x}$. From Eq. (10) written in the form

$$\bar{y}_s = [(2\xi)^{1/2}\,T_b/(\rho_s u_s^* T_s)]\,I(\eta_s) \quad (31)$$

and from the definition of $\bar{y}$ [Eq. (2a)] written in the form

$$\bar{y}_s = \int_0^{y_s^*} [(r_b + y^*\cos\theta_b)/L]^j\,dy^* = [(r_s + r_b)\,x^*\tan\theta_s/2Ly_s^*]^j y_s^* \quad (32)$$

we have upon elimination of $\bar{y}_s$ and the use of Eq. (14)

$$P_s = P_b = p_b/\rho_\infty U_\infty^2 = Q_1(j)\,Q_3(j)\,[(\gamma - 1)/2\gamma]\,(F/A) \quad (33)$$

where

$$Q_3(j) = \begin{cases} \cot\theta_s & \text{for } j = 0 \\ \dfrac{2(x^*/L)\cos\theta_b}{3[2 + (\tan\theta_s/\tan\theta_b)]\,(\tan\theta_s/\tan\theta_b)} & \text{for } j = 1 \end{cases} \quad (34)$$

and where

$$F = T_b I(\eta_s)/T_0 f(\eta_s) \quad (35)$$

Therefore, if from Eq. (16) a streamfunction $f(\eta)$ and its derivatives were to be known at $\eta = \eta_s$, the relations (27), (28), (30) and (33) would form a closed system of four equations in the four unknowns A, θ_s, D_s, and P_s.

IV. Method of Calculation

The model as formulated imposes the following restrictions on the input gas and body properties: M_∞ sufficiently large such that $c_p T_0 \approx U_\infty^2/2$, $T_b/T_0 \ll 1$, γ = constant, Pr = 1, and $\theta_b \ll 1$.

The solution for the viscous layer streamfunction $f(\eta)$ and for the various flow properties of interest proceeds by first transforming Eq. (16) to the following set of first-order differential equations as in Ref. 6:

$$f_\eta = J, \quad J_\eta = Z^{1/2}(1 + C_2 I)^{-1} g, \quad g_\eta = -Z^{1/2}(1 + C_2 I)^{-1} fg \quad (36)$$

where

$$Z = |1 - J|(1 + C_2 J) \equiv I_\eta \quad (37)$$

The no-slip boundary conditions

$$\begin{aligned} f(0) = J(0) = I(0) = 0 \quad &\text{at } \eta = 0 \\ J(\eta_s) = 1 \quad &\text{at } \eta = \eta_s \end{aligned} \quad (38)$$

are then imposed. Now, for values of the wall shear $g(0) = (f_{\eta\eta})_b$ greater than the value which gives an inviscid flow region at the outer edge of a boundary layer ($\eta_s \to \infty$), a velocity profile with finite shear $g(\eta_s) = (Nf_{\eta\eta})_s$ at the shock surface can be obtained for each station along the body within the merged layer. At each such value of $g(0)$, the no-slip boundary conditions are fully specified. Beginning then at $\eta = 0$ with a value $g(0) = [g(0)]^+_{\eta\to\infty}$ only slightly larger than the value $[g(0)]_{\eta\to\infty}$ which gives the boundary-layer solution ($\eta_s \to \infty$), Eqs. (36) and (37) are simultaneously integrated out from the body surface to the shock surface for fixed local values of C_1 and C_2. The initial guesses for these parameters are obtained from the boundary-layer limit $\eta_s \to \infty$ with θ_s guessed to be $\theta_s = \theta_{s_{inv}}$ where $\theta_{s_{inv}} = \theta_{s_{inv}}(\gamma, M_\infty, \theta_b, j)$ is the inviscid shock layer value for wedges and cones given in Ref. 12. As shown in the Appendix

$$C_1|_{\eta_s\to\infty} = (T_0/T_b)\,[\cos(\theta_{s_{inv}} + \theta_b)/\cos\theta_{s_{inv}}]^2 \quad (39)$$

$$C_2|_{\eta\to\infty} = 0 \quad (40)$$

The numerical integration of Eqs. (36) and (37) is stopped at the first point η reached within the viscous layer where $J = f_\eta = u^*/u_s^* \geqq 1$. The coordinate η_s is the finite value of η at this point, and the resulting finite values of $f(\eta_s)$, $g(\eta_s)$, and $I(\eta_s)$ are used to compute A and F in approximate form from [see Eq. (27)]

$$A = \left[\frac{\cos\theta_{s_{inv}}}{\cos(\theta_{s_{inv}} + \theta_b)} + \frac{2Q_1(j)\,Q_2(j)}{\sin 2(\theta_{s_{inv}} + \theta_b)}\left(\frac{g}{2f}\right)_{\eta=\eta_s} \right]^{-1} \quad (41)$$

and the relation given by Eq. (35). These results are then used to provide a better value of θ_s from Eqs. (28, 30, and 33). Better values for the local parameters C_1 and C_2 are next obtained from the relations (see Appendix)

$$C_1 = \frac{T_0}{T_b}\left\{ \frac{\cos\theta_s}{\cos(\theta_s + \theta_b)} + \frac{2Q_1(j)Q_2(j)}{\sin[2(\theta_s + \theta_b)]}\left(\frac{g}{2f}\right)_{\eta=\eta} \right\}^{-2} \quad (42)$$

$$C_2 = \frac{[2 + (\tan\theta_s/\tan\theta_b)](\tan\theta_s/\tan\theta_b)}{I(\eta_s)f(\eta_s)} \quad (43)$$

and beginning again at $\eta = 0$ with $g(0) = [g(0)]^+_{\eta\to\infty}$, Eqs. (36) and (37) are reintegrated from the body to the shock surface $\eta = \eta_s$. When after such successive iterations the results at the shock surface from one cycle agree sufficiently with those values from the previous cycle, the local no-slip viscous layer solution is available. The effects of small local velocity slip and temperature jump are then computed as local perturbations from the no-slip results. The method for obtaining the local slip solution is entirely analogous to that given in Ref. 6 except that Eqs. (39) and (40) of that reference are replaced by

$$\frac{u_{sl}^*}{u_s^*} = (f_\eta)_b \cong \left[\frac{\sin\theta_b}{(3L/x^*)}\right]\left[\left(1 - \frac{2j}{3}\right)Q_{3_{nsl}}(j)\right]^{-1}\left[\frac{\pi\gamma}{(\gamma - 1)}\,\frac{T_b}{T_0}\right]^{1/2} \cdot \left[\frac{A_{nsl}}{2f_{nsl}F_{nsl}}\right]_{\eta=\eta_s}[(f_{nsl})_{\eta\eta}]_{\eta=0} \quad (44)$$

$$A_{sl} \cong \left\{ \frac{\cos\theta_{s_{nsl}}}{\cos(\theta_{s_{nsl}} + \theta_b)} + \frac{f_{nsl}}{f}\left[\frac{1}{A_{nsl}} - \frac{\cos\theta_{s_{nsl}}}{\cos(\theta_{s_{nsl}} + \theta_b)}\right] \right\}^{-1}_{\eta=\eta_s} \quad (45)$$

and the rarefraction parameter [Eq. (35) of Ref. 6] is replaced by

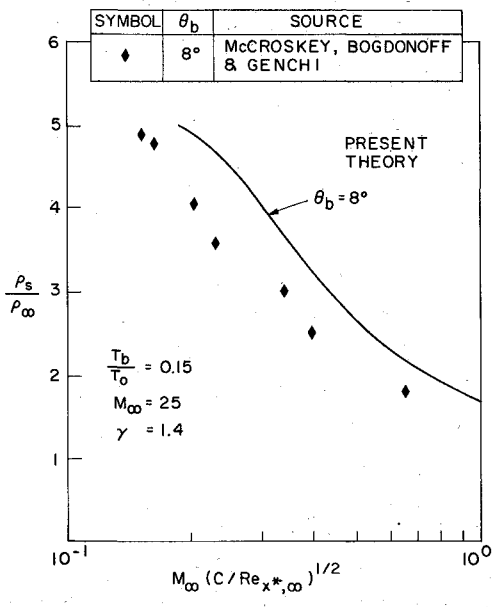

Fig. 2 Density ratio across the shock structure for a wedge.

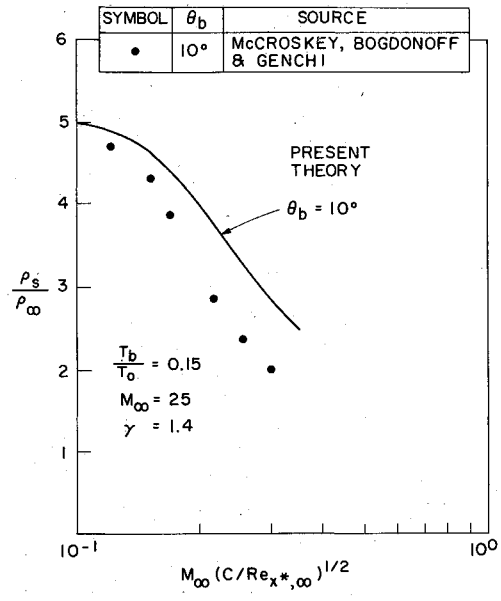

Fig. 3 Density ratio across the shock structure for a cone.

$$\frac{M_\infty C^{1/2}}{Re^{1/2}_{x^*,\infty}} = \left[\frac{Q_1(j)}{(1-2j/3)Q_3(j)(\gamma-1)F}\right]^{1/2}\left[\frac{x^*\sin\theta_b}{3L}\right]^j / f(\eta_s) \quad (46)$$

The final results at $g(0) = [g(0)]^+_{\eta_s\to\infty}$ constitute the local solution at the downstream end of the merged layer. The final values there for C_1 and C_2 become the initial guesses for these parameters at the adjacent station a small distance upstream. The viscous layer equations are integrated here from $\eta = 0$ with $g(0) = [g(0)]^+_{\eta_s\to\infty} + \Delta g(0)$, where $\Delta g(0)$ is a small increment in the surface shear $g(0)$. Through this stepwise upstream marching method, with successive iteration cycles at each step, the velocity and state variables are computed at several stations x^* within the merged layer regime. The computation is stopped at the upstream end when the condition $M_\infty\alpha \ll 1$ or the condition $(f_\eta)_b \ll 1$ is no longer satisfied. If the computation is carried to stations x^* farther upstream, the present model breaks down as the calculated values of ρ_s/ρ_∞ become less than unity. This occurs at values of the rarefaction parameter $M_\infty(C/Re_{x^*,\infty})^{1/2}$ of the order of unity.

VI. Results and Discussion

Computations have been carried out in the manner indicated in the previous section. The cases cover the range $20 \leqq M_\infty \leqq 25$, $0.06 \leqq T_b/T_0 \leqq 0.15$ *and* $0° \leqq \theta_b \leqq 20°$. Based on the parameters of the analysis, empirical correlation formulas may be used to represent the numerical results with an accuracy of 5%. The correlations obtained for wedges are

$$\frac{P_b\cos\theta_b}{\bar{\chi}_\infty(1+\frac{1}{2}(\cot\theta_s-\tan\theta_b)\sin 2\theta_b]} = 0.022 - 0.921\log_{10}\beta_w, \quad \beta_w < 1 \quad (47)$$

$$\frac{M^3_\infty St\cos\theta_b}{\bar{\chi}^{3/2}_\infty[1+\frac{1}{2}(\cot\theta_s-\tan\theta_b)\sin 2\theta_b]} = 0.001 - 0.037\log_{10}\beta_w, \quad \beta_w < 1 \quad (48)$$

where the modified rarefraction parameter

$$\beta_w = (T_b/T_0)^{1/2}\frac{M^2_\infty C}{Re_{x^*,\infty}[1+\frac{1}{2}(\cot\theta_s-\tan\theta_b)\sin 2\theta_b]} \quad (49)$$

reduces for $\theta_b = 0$ to the flat plate parameter given in Ref. 6. The correlations obtained for cones are

$$\log_{10}(P_b/\sin^2\theta_b) = 0.23\,[0.96 + 0.65\tanh(\log_{10}\beta_c - 2.1)], \quad \beta_c < 10^3 \quad (50)$$

$$\log_{10}\left[\frac{M^2_\infty St}{\bar{\chi}_\infty(1+\tan\theta_s/\tan\theta_b)^2\sin\theta_b}\right] = 0.36[1.1 - 0.92\tanh(\log_{10}\beta_c - 2.6)], \quad \beta_c < 10^3 \quad (51)$$

where

$$\beta_c = (T_b/T_c)^{1/2}(M^2_\infty C/Re_{x^*,\infty}\sin^4\theta_b) \quad (52)$$

is a modified rarefaction parameter proportional to the square of the usual conical correlation parameter $M_\infty C^{1/2}/Re^{1/2}_{x^*,\infty}\sin^2\theta_b$.

In Fig. 2, the density at the shock surface for a 8° wedge is compared with measured values obtained by McCroskey, Bogdonoff, and Genchi.[14] Considering the scatter in the data, the agreement with theory would appear to be good. The theoretical shock density ratio for a 10° cone is shown compared with the data in Fig. 3. In contrast with a wedge having the same flow conditions and comparable angle θ_b, the shock at the same distance x^* from the leading edge is weaker on the cone. This is due to the circumferential spreading of the flow around the cone, bringing the shock wave closer to the body surface and causing the merged layer to extend farther downstream than on the wedge.

Figure 4 presents the wedge surface pressures given by Vidal and Bartz[9] in comparison with the theory for several values of θ_b. The strong interaction and free molecule limits given by Hayes and Probstein[13] are also shown. Both the present theory and the data lie below the result predicted by strong interaction

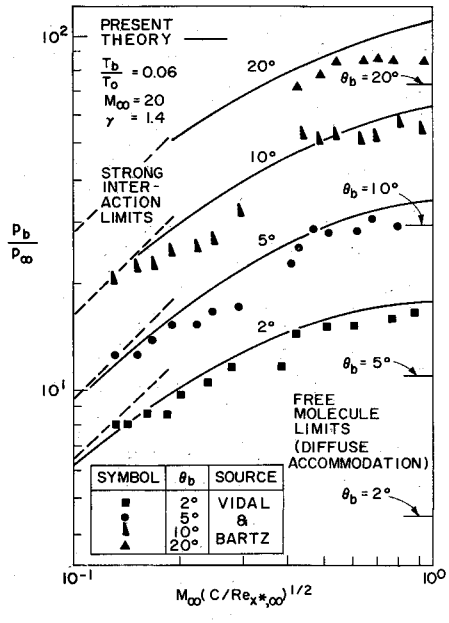

Fig. 4 Wall pressure on wedges.

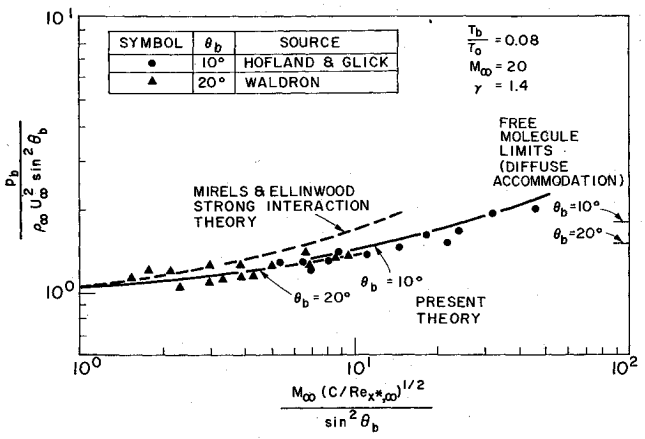

Fig. 5 Wall pressure on cones.

theory. This is also seen to be true for sharp cones as shown in Fig. 5 where the cone surface pressure by the present theory and by the strong interaction theory of Mirels and Ellinwood[19] are compared to the experimental data in the form presented by Waldron[17] and by Hofland and Glick.[18]

On Fig. 6, the experimental heat-transfer data obtained by Vidal and Bartz[9] on wedges is compared with the theory, and the agreement appears to be quite good. The theoretical result for cones is given in Fig. 7 compared to experiment in the form presented by Waldron.[17]

In view of the reasonable agreement of experimental data with the theory it would appear that the present continuum merged layer model is a satisfactory one up to rarefaction parameters $M_\infty(C/Re_{x^*,\infty})^{1/2} \sim 1$. This limit would correspond to distances back from the leading edge of the order of M_∞ mean free paths.

Appendix: The Parameters C_1 and C_2

By Eq. (27), the parameter C_1 is

$$C_1 = A^2 \frac{T_0}{T_b} = \frac{T_0}{T_b}\left\{\frac{\cos\theta_s}{\cos(\theta_s+\theta_b)} + \frac{2Q_1(j)\,Q_2(j)}{\sin[2(\theta_s+\theta_b)]}\left(\frac{g}{2f}\right)_{\eta=\eta_s}\right\}^{-2} \quad \text{(A1)}$$

To find C_2, an expression for the parameter $M_\infty\alpha$ is first required. To obtain this, we eliminate ξ between Eqs. (6) and (14) for the case of $j = 1$ and note that $\rho_b\mu_b/\rho_\infty\mu_\infty = \gamma M_\infty P_s 2T_0/(\gamma-1)T_b^{1/2}$ from $\mu \sim T^{1/2}$ and the equation of state, with the result

$$M_\infty\alpha = \frac{3\cos\theta_b(\tan\theta_s+\tan\theta_b)[1+(\tan\theta_s/\tan\theta_b)]^2}{8\gamma P_s A f^2(\eta_s)} \cdot\{[(\gamma-1)/2](T_b/T_0)\}^{1/2} \quad \text{(A2)}$$

Using Eqs. (22 and 33–35) to eliminate P_s, we obtain then

$$C_2 = [2+(\tan\theta_s/\tan\theta_b)](\tan\theta_s/\tan\theta_b)/I(\eta_s)f(\eta_s) \quad \text{(A3)}$$

from Eq. (17b).

In the boundary-layer limit $\eta_s \to \infty$ and $g(\eta_s) \to 0$, we find that since $f_\eta \sim 1$ when $\eta \sim \eta_s$

$$[f(\eta_s)]|_{\eta_s\to\infty} = \left[\int_0^{\eta_s} f_\eta d\eta\right]_{\eta_s\to\infty} \to \infty \quad \text{(A4)}$$

$$[I(\eta_s)]|_{\eta_s\to\infty} = \left[\int_0^{\eta_s}(1-f_\eta)(1+C_1 f_\eta)\,d\eta\right]_{\eta_s\to\infty} = \text{finite} \quad \text{(A5)}$$

so that taking $\theta_s = \theta_{s_{inv}}$, Eqs. (A1) and (A3) yield

$$C_1|_{\eta_s\to\infty} = (T_0/T_b)[\cos(\theta_{s_{inv}}+\theta_b)/\cos\theta_{s_{inv}}]^2 \quad \text{(A6)}$$

$$C_2|_{\eta_s\to\infty} = 0 \quad \text{(A7)}$$

Here $\theta_{s_{inv}}(\gamma, M_\infty, \theta_b, j)$ is the inviscid shock layer value for θ_s obtained from Ref. 12.

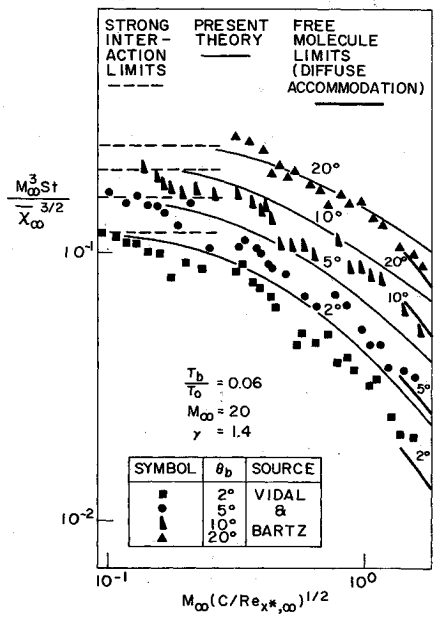

Fig. 6 Heat-transfer rate on wedges.

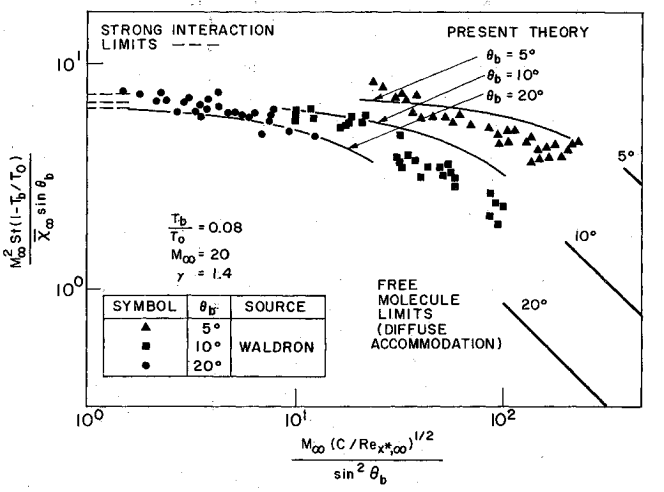

Fig. 7 Heat-transfer rate on cones.

References

[1] Rubin, S. C., Lin, T. C., Pierucci, M., and Rudman, S., "Hypersonic Interactions Near Sharp Leading Edges," *AIAA Journal*, Vol. 7, No. 9, Sept. 1969, pp. 1744-1751.

[2] Cheng, H. K., Chen, S. Y., Mobly, R., and Huber, C., "On the Hypersonic Leading-Edge Problem in the Merged Layer Regime," *Rarefield Gas Dynamics*, Supplement 5, Vol. I, edited by L. Trilling and H. Wachman, Academic Press, New York, 1969, pp. 451–463.

[3] Novack, B. B. and Cheng, M. K., "Numerical Analysis and Modeling of Slip Flows at Very High Mach Numbers," *Lecture Notes in Physics, No. 8*, Proceedings Second International Conference on Numerical Methods, Springer Verlag, Heidelburg, 1971.

[4] Pan, Y. S. and Probstein, R. F., "Rarefied Flow Transition at a Leading Edge," *Fundamental Phenomena in Hypersonic Flow*, Cornell University Press, Ithaca, N. Y., 1966, pp. 259–306.

[5] Oguchi, H., "Shock Wave and Viscous Layer Structure in a Rarefied Hypersonic Flow Near the Leading Edge of a Sharp Flat Plate," Rept. 418, 1967, Inst. of Space and Aeronautical Sciences, Univ. of Tokyo, Tokyo, Japan.

[6] Shorenstein, M. L. and Probstein, R. F., "The Hypersonic Leading Edge Problem," *AIAA Journal*, Vol. 6, No. 10, Oct. 1868, pp. 1898–1906.

[7] McCroskey, W. J., Bogdonoff, S. M., and McDougall, J. G., "An Experimental Model for the Sharp Flat Plate in Rarefied Hypersonic Flow," *AIAA Journal*, Vol. 4, No. 9, Sept. 1966, pp. 1580–1587.

[8] Harbour, P. J. and Lewis, J. H., "Preliminary Measurements of the Hypersonic Rarefied Flow Field on a Sharp Flat Plate Using an Electron Beam Probe," *Rarefied Gas Dynamics*, Supplement 4, Vol. II, edited by C. L. Brundin, Academic Press, New York, 1967, pp. 1031–1046.

[9] Vidal, R. J. and Bartz, J. A., "Surface Measurements on Sharp Flat Plates and Wedges in Low Density Hypersonic Flow," CAL AF-2041-A-2, 1968, Cornell Aeronautical Lab., Buffalo, N. Y.

[10] Probstein, R. F. and Elliott, D., "The Transverse Curvature Effect in Compressible Axially Symmetric Laminar Boundary Layer Flow," *Journal of the Aeronautical Sciences*, Vol. 23, No. 3, March 1956, p. 208.

[11] Oguchi, H., "Leading Edge Slip Effects in Rarefied Hypersonic Flow," *Rarefied Gas Dynamics*, Supplement 2, Vol. II, edited by J. A. Laurmann, Academic Press, New York, 1963, pp. 181–193.

[12] TR 1135, 1953, NACA.

[13] Hayes, W. D. and Probstein, R. F., *Hypersonic Flow Theory*, Academic Press, New York, 1959.

[14] McCroskey, W. J., Bogdonoff, S. M., and Genchi, A. P., "Leading Edge Flow Studies of Sharp Bodies in Rarefied Hypersonic Flow," *Rarefied Gas Dynamics*, Supplement 4, Vol. II, edited by C. L. Brundin, Academic Press, New York, 1967, pp. 1047–1066.

[15] Vas, I. E., Iacavazzi, C., Carlomagno, G., and Bogdonoff, S. M., "Effect of Body Inclination on the Merging of a Hypersonic Low Density Flow Over Sharp Two-Dimensional Linear Bodies," *Rarefied Gas Dynamics*, Supplement 5, Vol. I, edited by L. Trilling and H. Wachman, Academic Press, New York, 1969, pp. 501–508.

[16] Feik, R. A., Genchi, A. and Vas, I. E., "A Study of Merging on Cones," *Rarefied Gas Dynamics*, Supplement 5, Vol. I, edited by L. Trilling and H. Wachman, Academic Press, New York, 1969, pp. 493–499.

[17] Waldron, H. F., "Viscous Hypersonic Flow Over Pointed Cones at Low Reynolds Numbers," *AIAA Journal*, Vol. 5, No. 2, Feb. 1967, pp. 208–218.

[18] Hofland, R. and Glick, H. S., "Low Density Hypersonic Flow Over a Cone," *AIAA Journal*, Vol. 8, No. 1, Jan. 1970, pp. 52–59.

[19] Mirels, H. and Ellinwood, J. W., "Hypersonic Viscous Interaction Theory for Slender Axisymmetric Bodies," *AIAA Journal*, Vol. 6, No. 11, Nov. 1968, pp. 2061–2070.

SEPTEMBER 1972 AIAA JOURNAL VOL. 10, NO. 9

Jet Impingement under VTOL Aircraft

THOMAS M. HOULIHAN* AND CHARLES D. THOMPSON†
Naval Postgraduate School, Montery, Calif.

A previous analytical solution for the flowfield beneath a VTOL model was extended to include tilted jet configurations. Additionally, a laboratory model was constructed to test the effects of variation in the parameters governing the flow. Free streamline profiles, pressure coefficients on the "ground" and "fuselage" of the apparatus and velocity profiles in the nozzles were determined from hot wire anemometer traverses of the flowfield. Experimental data compared favorably with theoretical determinations over the flow regions tested.

Nomenclature

C_p = pressure coefficient
K = complete elliptic integral of the first kind
K' = defined by $K'(k) \equiv K(k')$
k = modulus of elliptic integral
k' = defined as $(1 - k^2)^{1/2}$
R_e = Reynolds number, $\Delta V_0/\nu$
T = complex variable in T-plane, $\xi + i\eta$
V_I = velocity at nozzle exit
$\bar{V}_I$ = average velocity at nozzle exit
V_0 = velocity along free streamlines
W = complex potential, $\Phi + i\Psi$
x, y = coordinates in physical plane
z = complex variable, $x + iy$
α = tilt angle of nozzle
β = plate angle
Γ = flow region in the T-plane
Δ = width of nozzle
δ_L, δ_R = asymptotic widths of streams flowing to left and to right
ζ = complex conjugate velocity, $u - iv$
θ = theta-function
ξ, η = coordinates of T-plane
ρ = density
Φ = velocity potential
Ψ = stream function

Subscripts
A, G, H = refer to stagnation points
F = refers to point on fuselage plate
r = refers to boundary point

Introduction

IN recent years, crowded airport facilities, the search for rapid urban transportation, and the need for military aircraft capable of operating from advanced bases, have resulted in a great deal of attention being given to VTOL aircraft. Much research has been performed on various models and full-scale versions of these aircraft. Some operational types have been developed.

When operating near the ground, these aircraft are quite similar in principle to ground effect machines. Ground effect can be either beneficial or detrimental, depending upon the configuration of the aircraft. Land erosion, damage to objects near the operating area, and recirculation of debris and hot exhaust gases beneath the fuselage are some of the problems involved with hovering near the ground. The reingestion of exhaust gases reduces the efficiency of the engines. Recirculating debris may also enter the engines or severely damage the underside of the aircraft. Some pilots have experienced handling difficulties, drastic loss of power, and visibility problems, as a result of ground effect.

The recirculating flow underneath the aircraft, however, can also produce a lifting force which can significantly reduce the thrust necessary to operate the aircraft. Small modifications to the aircraft, such as tilting of engines, can often reduce the unfavorable effects to such an extent that the additional lift provided by the recirculating flow can produce improved performance. In order to estimate the effects of various modifications, a mathematical model of the flowfield beneath VTOL aircraft, incorporating the elements of free streamline theory, was developed. Verification of the primary conclusions of this analysis, together with an investigation of the range of its applicability, is the subject of the following work.

Theoretical Analysis

A theoretical solution to the flowfield beneath a VTOL aircraft was obtained by Goldstein and Siegel.[1] Their determinations for a two-dimensional model of an aircraft with a slot-jet nozzle exhaust in each wing featured a steady, incompressible, inviscid fluid flow. A flat plate at an angle to the vertical represented the "fuselage" in the configuration shown in Fig. 1 and the nozzles were assumed to always be perpendicular to the

Received December 28, 1970; revision received March 20, 1972. Index category: VTOL Aerodynamics.

* Assistant Professor, Department of Mechanical Engineering. Member AIAA.

† Lieutenant, U. S. Navy, Pensacola, Fla.